EASR

Engineering and Applied Science Research

https://www.tci-thaijo.org/index.php/easr/index

Published by the Faculty of Engineering, Khon Kaen University, Thailand

Grain growth kinetics and hardness empirical model of 253 MA austenitic stainless steel after multi-pass cold rolling

Rana K. Melinia[1)], Moch. Syaiful Anwar[1, 2)], Robert R. Wijaya[3)] and Eddy S. Siradj*[1)]

[1)]Department of Metallurgical and Materials Engineering, Faculty of Engineering, Universitas Indonesia, Kampus UI Depok, Jawa Barat 16424, Indonesia
[2)]Research Center for Metallurgy and Materials, Indonesian Institute of Sciences, Kawasan PUSPIPTEK Gedung 470, Tangerang Selatan, Banten 15314, Indonesia
[3)]Research Center for Chemistry, Indonesian Institute of Sciences, Kawasan PUSPIPTEK Gedung 452, Tangerang Selatan, Banten 15314, Indonesia

Received 16 August 2021
Revised 26 October 2021
Accepted 5 November 2021

Abstract

This study investigated changes in the average grain size and hardness values of 253 MA austenitic stainless steel (ASS) and determined the grain growth kinetics as well as a hardness empirical model. A 35% multi-pass cold rolling process was employed to reduce the thickness of a 253 MA austenitic stainless steel pipe. Then, the rolled steel was annealed at 1100 °C for various soaking times of 0, 900, 1800, 2700, and 3600 s in a tubular furnace under a hydrogen atmosphere, followed by quenching to room temperature in the cool zone of the furnace. Then, micro-Vickers hardness measurements were done using a force of 0.3 N and the grain size changes were observed. A line intercept method was applied to measure the change of the 253 MA austenitic grain size. The results show that the average grain size of 253 MA ASS (austenitic stainless steel) increased with soaking time, while the hardness values decreased. Additionally, an equation modeling the predicted grain growth and hardness values was obtained.

Keywords: 253 MA Austenitic stainless steel, Grain size, Grain growth, Micro-Vickers hardness, Empirical model

1. Introduction

Sandvik 253 MA steel is an austenitic stainless steel with a chromium-nickel alloy combined with N, Mn, Si and Ce [1]. This steel is very suitable for various applications that require high operating temperatures, such as fluidized bed risers, anchor refractories, and reformer tubes, among other applications [2-4]. The steel usually undergoes a heat treatment to obtain a material with better quality before being marketed to users. The microstructural and mechanical properties of the steel are changed after heat treatment [5]. These changes have an effect on steel grain growth over time, allowing steel grains to grow from fine to coarser sizes. A fine grain diameter is better as smaller grains can increase grain boundaries areas to prevent dislocation movements [6].

Numerous studies of grain growth in steel have been done. Lin Xie et al. investigated the effect of the grain size of a duplex Fe-23Cr-8.5Ni alloy on the mechanical behavior of steel [6]. The alloy's phases consist of ferrite and austenite after cold rolling and annealing. The grain sizes of both phases increased with annealing time, resulting in decreased yield strength and improved ductility. H.C. Ji et al. conducted a static grain growth experiment of 21-4N heat resistant steel using a solution treatment at various temperatures over the range of 1000-1180 °C with holding times of 0 and 40 min [7]. They found that the grain size reaches stable values due to the effects of undissolved metal carbide (M23C6) and pinning around grain boundaries at temperatures below 1120 °C. Grains become coarser at 1120 °C and higher temperatures because of the effect of large amounts dissolved M23C6 and weak pinning on austenite grains. A.T. Krawczynska et al. studied the effects of hydrostatic pressures greater than 2 GPa on recrystallization and grain growth in nanostructured austenitic stainless steel 316LVM [8]. Nanograined austenite of 316LVM stainless steel was successfully obtained by profile rolling (PR) and high-pressure torsion (HPT) methods and annealed under hydrostatic pressure. They found the grain size of PR sample, which has a low angle boundary, was finer than the grain size of HPT sample after annealing under hydrostatic pressure. Z. Nasiri et al. reviewed the thermal mechanism of microstructural refinement in steels, which include thermal cycling, martensite process, and static recrystallization (SRX) [9]. M. Naghizadeh and H. Mirzadeh investigated microstructural evolution during annealing of plastically deformed AISI 304 austenitic stainless steel [10]. They found that higher annealing temperatures resulted in more rapid reversion and recrystallization, and the grain sizes were coarse with increasing annealing temperature and soaking time. Furthermore, the hardness values decline after the annealed process. M.J. Sohrabi et al. reviewed deformation-induced martensitic transformation, the transformation-induced plasticity (TRIP) effect, and reversion annealing in metastable austenitic stainless steels [11]. They showed that the presence of Mo in AISI 316L halted martensitic reversion, recrystallization and grain growth. A. Järvenpää et al. investigated the effect of nitride precipitation on the mechanical stability of grain-refined austenitic structures obtained during reversion annealing in 310NL steel [12]. They found that nitride precipitation occurred during annealing at temperatures above 750 °C that resulted in

*Corresponding author. Tel.: +62 817 6767 019
Email address: siradj@metal.ui.ac.id
doi: 10.14456/easr.2022.43

slightly increased grain sizes and decreased yield strength. A. Järvenpää et al. reviewed the processing and properties of reversion-treated austenitic stainless steels [13]. They indicated that the grain size refinement was more efficiently obtained from austenite formed from cell-type martensite than from lath-type martensite. M. Tikhonova et al. investigated static grain growth in an austenitic stainless steel subjected to intense plastic strain [14]. Multidirectional hot forging was employed to refine the grain size of S304H austenitic stainless steel. The grain growth of this steel increased with annealing time after multidirectional forging at low temperatures. M. Naghizadeh and H. Mirzadeh studied the effects of various alloying elements in 304, 304L and 316L austenitic stainless steels at elevated temperatures [15]. They found that carbon resulted in slightly coarser grains, but the molybdenum content significantly impeded grain development at higher temperatures. J.K. Stanley and A.J. Perrotta compared the grain growth characteristics for AISI Type 304, 316, 321, and 347 stainless steel after rapid heating and cooling [16]. They found the grain growth behaviour of Types 321 and 347 steels were similar, while those of Types 304 and 316 were not. D. Dong et al. developed a pragmatic model to predict austenite grain growth in a SA508-III nuclear reactor pressure vessel steel. They stated that with increased annealing temperature, second-phase particles tend to dissolve and the pinning effects become smaller, which results in a rapid grain growth [17].

To the best of our knowledge, there is no such study of 253 MA ASS steel. This research aimed to determine the changes in the average grain size and hardness values of 253 MA ASS during grain growth. The empirical model of Sellars is used to predict grain growth of 253 MA ASS, while Hall-Petch model can be used to predict hardness of 253 MA ASS.

2. Materials and methods

2.1 Materials and instruments

Multi-pass cold rolling was done at room temperature under laboratory conditions. The technical specifications of the roll machine used in the current study are shown in Table 1. The chemical composition of the 253 MA ASS was analyzed using optical emission spectroscopy (OES) with a Bruker AXS. The results are summarized in Table 2. Annealing was done in a horizontal tube furnace manufactured by Nabertherm GmbH RSH 50 using a type N thermocouple at 1100 ℃ with soaking times of 0, 900, 1800, 2700, and 3600 s. There is one heating zone in the furnace chamber. The thermocouple was positioned outside the working tube between the heating wires to measure temperature in the furnace. A Nabertherm 410 series controller was employed to adjust temperature and time for the annealing process. This study employed an Olympus optical microscope to observe specimen microstructure and a Micro Vickers Hardness tester, manufactured by Mitutoyo using a force of 0.3 N to determine hardness. The current work used a 200 mm long 253 MA ASS pipe with an outside diameter of 60.33 mm.

Table 1 Technical specification of roll machine

Item	Specification
Roller diameter	Φ 210 mm
Power	55-75 kW
Center Distance Between Gears	650 mm
Rolling Speed	1.5-2 m/s
Cutting Length	1.5-12 m

Table 2 Chemical composition of 253 MA ASS pipe (wt%)

C	Si	Mn	P	S	Cr	Ni	N	Ce	La	Fe
0.079	1.422	0.51	0.03	<0.005	22.06	10.86	0.384	0.03	0.014	Bal.

2.2 Methods

A 253 MA ASS pipe was prepared with dimensions of 100 mm x 10 mm x 3.28 mm using an EDM-wire cutting process to serve as a sample plate. Then, the cold rolling process was conducted. An illustration of sample preparation and cold rolling is presented in Figure 1.

A multi-pass cold rolling process was done ten times on a roller plate sample to maintain the rectangular shape of sample until a deformation reduction of 35% was achieved with a final thickness of approximately 2.32 mm. However, the sample shape became curved at the 8^{th} and 10^{th} passes, resulting a reduction of the sample length. The 10^{th} pass showed this to a greater degree than the 8^{th} sample. Alternatively, strain-induced martensite formation during cold rolling was an obstacle in the reduction of sample thicknesses. The reduction at each pass is shown in Table 3.

Table 3 Reduction of 253 MA ASS plate thickness by multi-pass cold rolling

Pass	Avg. thickness (mm)	Length (mm)	Reduction of thickness (%)
0	3.28	100	0
1	2.76	118.96	17
2	2.70	121.6	20
3	2.51	130.81	27
4	2.45	134.01	29
5	2.39	137.19	32
6	2.37	138.73	33
7	2.34	140.31	34
8	2.35	139.72	33
9	2.34	140.51	34
10	2.32	132.22	35

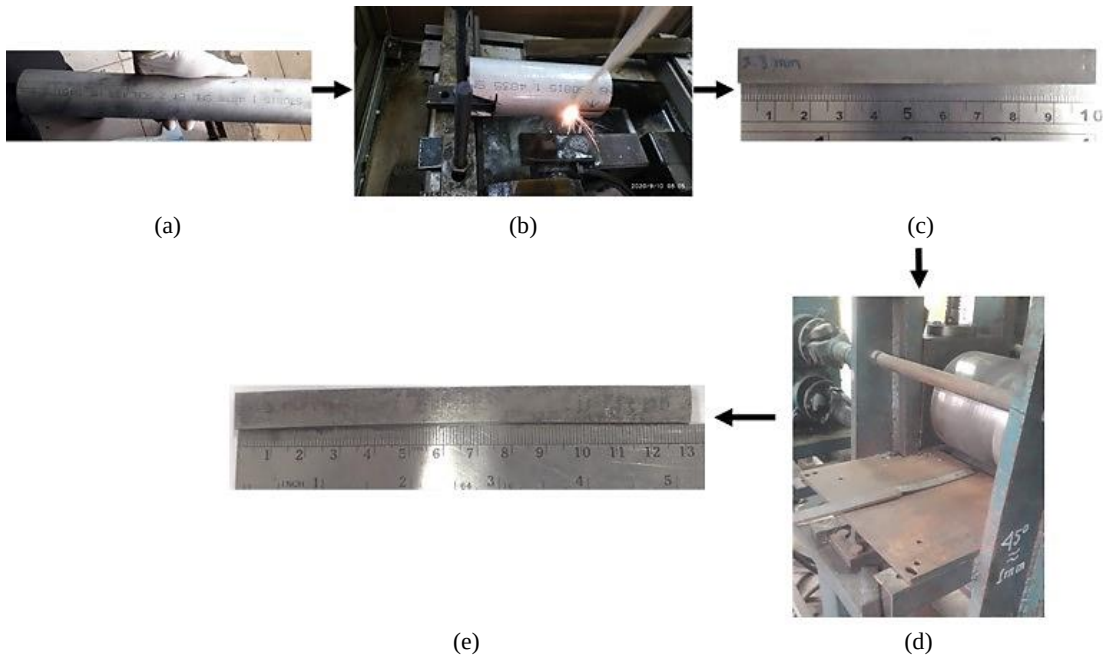

Figure 1 Sample preparation and its subsequent cold rolling process: (a) 253 MA ASS pipe, (b) EDM wire cutting process, (c) sample before cold rolling with an initial length of 100 mm and thickness of 3.28 mm, (d) cold rolling process, and (e) sample after cold rolling with a final length of 132 mm and thickness of 2.32 mm.

After that, the rolled samples were cut into five plates. The samples were heat-treated, increasing the temperature from room temperature to 1100 ℃ in a tubular furnace with a heating rate of 5℃/min and soaking times of 900, 1800, 2700, and 3600 s. A quenching process was done by switching the samples from the hot zone to cool zone until room temperature was achieved. The annealing and quenching processes were done under a hydrogen atmosphere to avoid oxide formation on the steel surfaces. The annealed samples with various soaking times of 0, 900, 1800, 2700, and 3600 s were compared to investigate the growth kinetics of austenite grains and the hardness of the 253 MA ASS samples. The sample with no heat soaking was immediate quenched after annealing. It was used as a control in the examination of the effects of heat soaking on grain growth and hardness. The thermal cycle of the experimental grain growth process is shown in Figure 2.

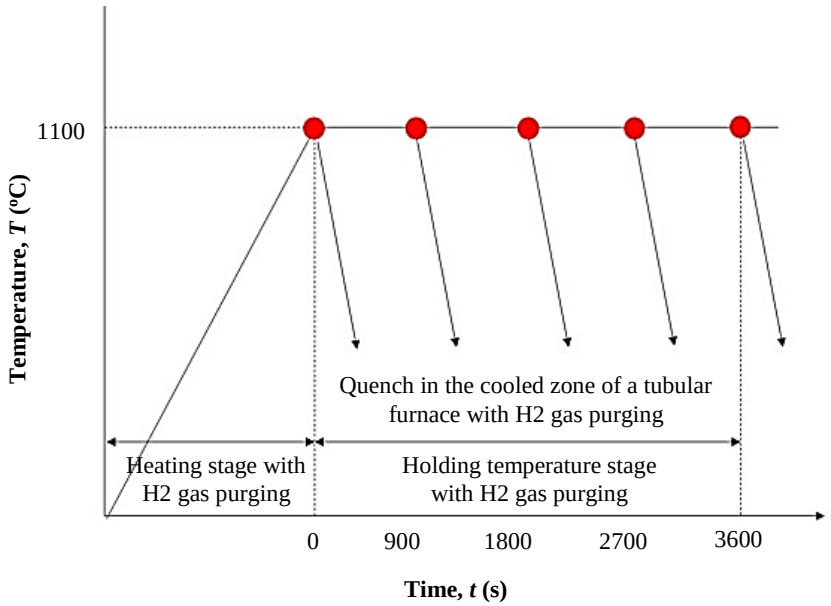

Figure 2 Thermal cycle of the experimental grain growth process.

After the heat treatment process, the quenched samples were polished and etched in a solution containing four parts of HCl and one part of HNO_3 on a volume basis, for about 18 s to reveal austenite grain boundaries. All procedures followed the guidelines of grain diameter standards of the American Society for Testing and Materials (ASTM). The actual austenite grain diameters were measured following ASTM E112 using a line intercept method. Grain diameters were estimated using the Sellars model [18]. Microstructural observations of samples and hardness tests were done in rolling direction (RD) sections. Figure 3 shows an illustration of the position where the sample for microstructural observations and hardness test was taken. The hardness values were estimated using the Hall-Petch model [19, 20].

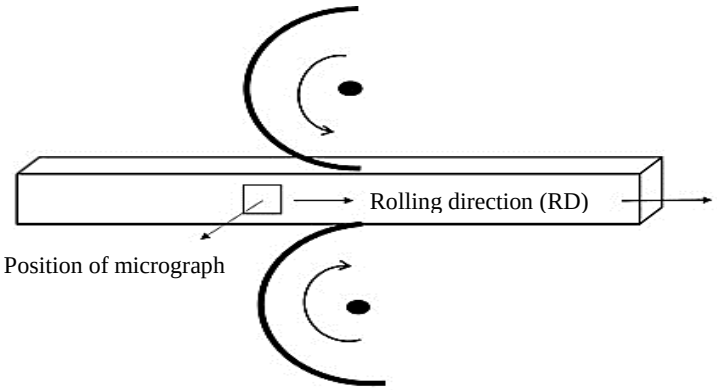

Figure 3 Illustration the position where microstructural observations were made and hardness test.

3. Results and discussion

3.1 Microstructural observations

Figures 4(a-f) show the microstructure of 253 MA ASS after multi-pass cold rolling as well as the isothermal annealing process at a temperature of 1100 ℃ with various soaking times. The deformation twin and martensite phases appeared to a slight degree in the microstructure due to plastic deformation during cold rolling [21, 22] as shown in Figure 4(a). The martensite phase changes to an austenite phase, and the deformation twin became the annealing twin in the austenitic grains due to recrystallization and grain growth during the annealing process. According to the growth accident model, the rapid rate of grain boundary migration during recrystallization forms annealing twins more quickly [23]. After complete recrystallization, austenite grains grow with increasing soaking time and became coarser, as shown in Figures 4(b-f). This impacted the decreased the yield and ultimate strength of the steel [24]. However, the incremental changes of austenite grain size of the steel are not significant during annealing, as shown in Table 4. This is probably due to the pinning effect of carbon. It precipitated in the austenitic grain, impeding grain growth, as shown in Figures 4(b-f). This might be main reason why the austenite grain size of the steel is quite stable during the annealing process. The effect of an alloying element on the austenitic grain size of steel was studied in earlier research [15].

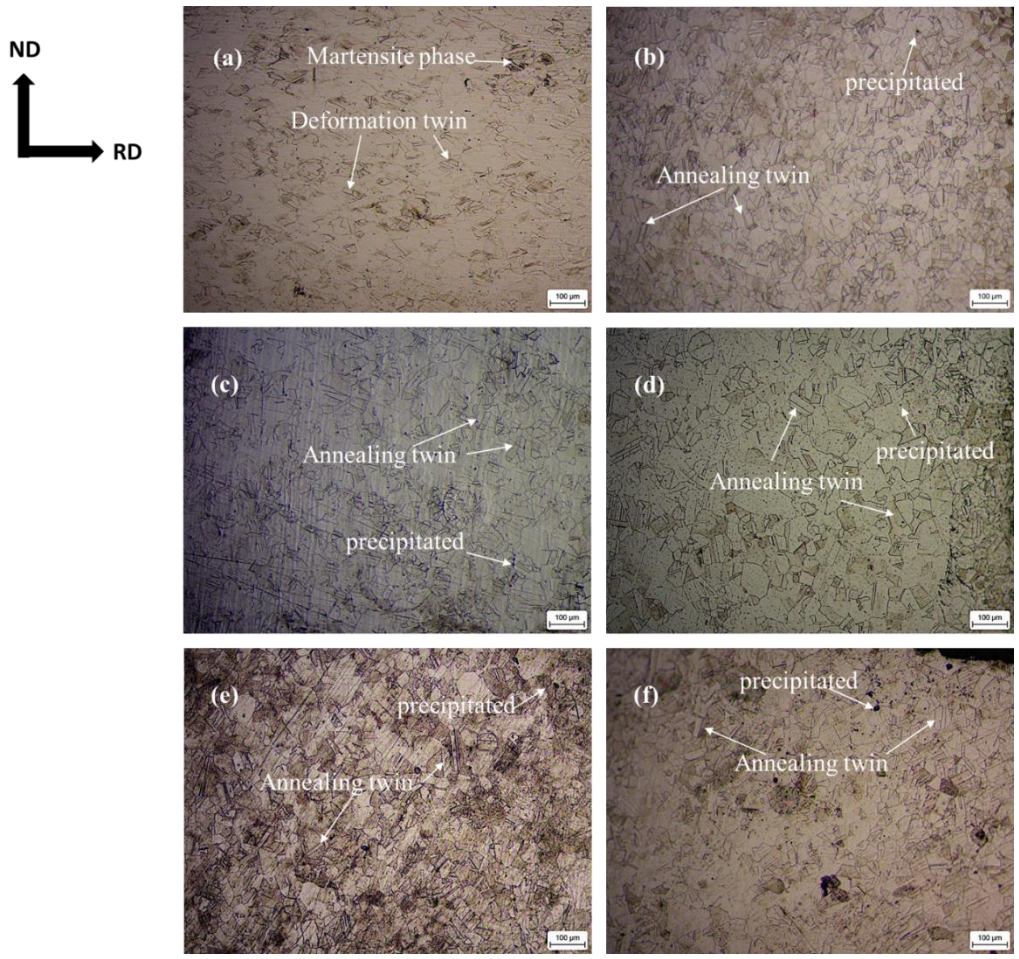

Figure 4 (a-f). Micrographs of 253 MA ASS sample after (a) multi-pass cold rolling, and annealing at 1100 ℃ for duration of (b) 0 s, (c) 900 s, (d) 1800 s, (e) 2700 s, (f) 3600 s taken from rolling direction (RD) section and at a 100X magnification.

3.2 Grain growth and its prediction in 253 MA austenitic stainless steel

Table 4 shows the average grain diameters of 253 MA ASS after various soaking times at 1100 °C. Grain diameter slightly increases with soaking times up to 3600 s. The incremental increase in the grain diameter for each soaking time at 1100 °C is given as 31% (0-900 s), 12% (900-1800 s), 5.3% (1800-2700 s), and 20% (2700- 3600 s). These values indicated there are several factors that cause austenitic grain growth to increase slowly. Micro alloying with Ce causes its precipitation in the austenite grain leading to the pinning effect at the grain boundary, inhibiting grain growth. The effect of the micro-alloying element on the grain growth process was examined in previous studies [13, 25]. Higher nitrogen contents resulted in sluggish grain growth in the steel. The material in the present work has a large nitrogen content compared with previous studies. Grain sizes of the current work are finer than in previous studies at the same annealing temperatures and soaking times. Previous studies were unclear about the degree of reduction in deformation experienced in 316LN stainless steel [26]. Then, higher chrome, nickel, and cerium contents in the steel might also contribute to impeding grain growth.

Table 4 Average grain diameter after annealing at 1100 ℃ with various soaking times

Soaking time (s)	0	900	1800	2700	3600
Average grain diameter (μm)	13	17	19	20	24

The grain growth of austenite 253 MA occurs spontaneously and grows constantly with increasing temperature and soaking time. Currently, the Sellars model is generally used to predict the growth of austenite grains [18]. The average grain diameter can be calculated using Equation (1) at specific temperatures and soaking times.

$$d^n - {d_0}^n = K \cdot t \tag{1}$$

where d is the average grain diameter, d_0 represents the initial grain diameter, n is a constant exponent for grain growth kinetics, t is soaking time, and K is a constant.

The constant K can be calculated using Equation 2.

$$K = k_0 \, EXP\left(-\frac{Q}{RT}\right) \tag{2}$$

where k_0 is a constant, T represents the specific heating temperature in Kelvin, R is the universal gas constant, 8.31 J/(mol•K), and Q is the activation energy for grain growth (J/mol).

The values of the constants n, K, and Q in the Sellars model depend on the metal types undergoing the grain growth process. Multiple regression was used to obtain the coefficient values using the Solver package in Microsoft Excel software.

Fitting of multiple variables using non-linear regression in Equations (1) and (2) was performed to determine the optimal values of n (2.52) and K (0.62). In the present study, the n value of 2.52 is close to value reported previous studies [15, 27, 28]. This means that after recrystallization is complete at around 3 to 8 s [18], the austenite grains of 253 MA ASS grow normally. This n value, 2.52, is sligthly larger than that reported for a pure metal, 2, suggesting that chemical segregation and solute drag play major roles in slowing grain growth [29]. Then, microalloying with Ce at 0.33 wt.% in 253 MA ASS resulted in retardation of grain growth kinetics.

The experimental and predicted grain diameter values are presented in Figure 5. This figure shows that predicted and experimental values are close, showing 1-4% of error. The Sellars model was used predict the austenite grain growth of 253 MA stainless steel, calculated using Equation (3).

$$d = \left(0.623 \cdot t + {d_0}^{2.52}\right)^{1/2.52} \tag{3}$$

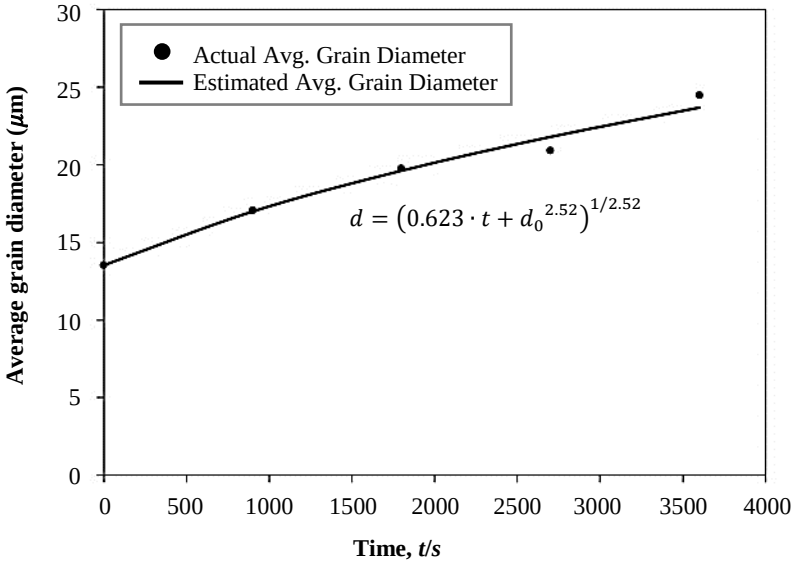

Figure 5 Comparison of the actual and estimated values of average grain diameter using the Sellars model.

3.3 Hardness and its prediction

Figure 6 shows the micro-Vickers hardness values vs. soaking time. Increased soaking time reduces micro-Vickers hardness values. This indicates that annealing at a specific temperature for a long time produces softer 253 MA stainless steel.

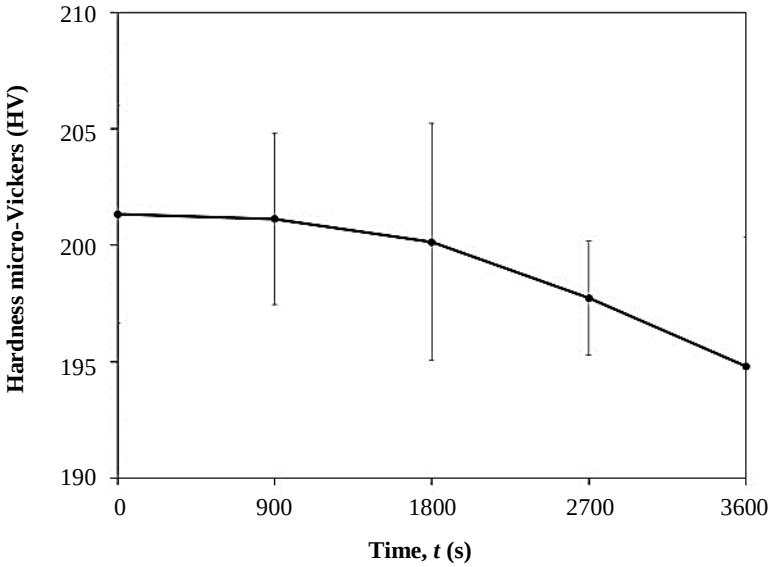

Figure 6 253 MA ASS hardness after various soaking times.

Figure 7 shows the effects of the average grain diameter on the resulting hardness values. The highest hardness is 201.3 HV with an average grain diameter of 13.54 µm. Alternatively, the lowest hardness was 194.8 HV with an average grain diameter of 24.5 µm. This figure shows that hardness decreases with increasing grain diameter. Samples with increased grain diameters have reduced area at the grain boundaries.

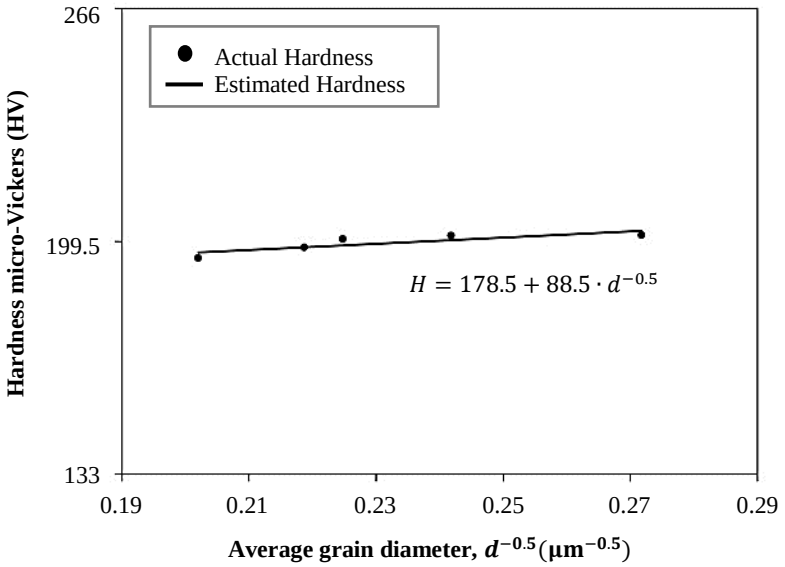

Figure 7 Comparison experimental and estimated micro-Vickers hardness values and estimated Hall-Petch values.

The Hall-Petch model was used to calculate the relationship between hardness values and grain growth. The H0 and k' coefficients were calculated using Equation (4) [19, 20].

$$H = H_0 + k' \cdot d^{-1/2} \quad (4)$$

where H_0 is the intrinsic hardness of 253 MA ASS, k' represents the Hall-Petch coefficient, and d is the average grain diameter.

Fitting multiple variables using non-linear regression in Equation (4) was performed to determine the optimal value of H_0 (178.5) and k' (88.5). The experimental and predicted hardness values are presented in Figure 7. This figure shows that the predicted and experimental values are close, with a 1% error. These findings indicates that the Hall-Petch model can predict the hardness values of 253 MA ASS using Equation (5).

$$H = 178.5 + 88.5 \cdot d^{-0.5} \quad (5)$$

4. Conclusions

This research concludes with four major points:

1. After the annealing process, the grain diameter of 253 MA ASS increases with the soaking time. This condition occurs because a greater amount of heat increases the grain boundary displacement and merges smaller grains into larger ones.

2. The grain growth process of 253 MA ASS proceeds normally with sluggish growth due to high Cr, Ni and N contents, the pinning effect of C and Ce elements and chemical segregation.

3. A model for predicting austenite 253 MA steel grain growth under various soaking times was obtained and the predicted results agree well with measured values.

4. According to the Hall-Petch model, the hardness value of 253 MA steel increased with decreased grain diameters and the predicted result agree well with measured values.

5. Acknowledgements

The authors would like to express their gratitude to the National Research and Innovation Agency Indonesia of the Ministry of Research and Technology and the Indonesian Institute of Sciences (LIPI) for financially supporting the PUTI Doktor with contract number NKB 3355/UN2.RST/HKP.05.00/2020, and LIPI research with contract number SK 197/H/2019. Moreover, the researchers thank PT. Cahaya Bina Baja-Sandvik for supporting the procurement of 253 MA stainless steel.

6. References

[1] Material.Sandvik/en/ [Internet]. Sweden: Sandvik AB; 2000-20011 [update 2021 Apr 22; cited 2020 Apr 2020]. Available from: https://www.materials.sandvik/en/materials-center/material-datasheets/ tube-and-pipe seamless/sandvik-253-ma/.

[2] Qiu X, Duan L, Duan Y, Li B, Lu D, Zhao C. Ash deposition during pressurized oxy-fuel combustion of Zhundong coal in a lab-scale fluidized bed. Fuel Process Technol. 2020;204:106411.

[3] Etienne J, Metcalfe RG. Stress corrosion cracking of stainless steel refractory anchors prior to service. J Fail Anal and Preven. 2018;18:8-12.

[4] Sanchez JJB, Marron BS, Garcia-Orta VG, Ruiz JCS, inventors. Steam-reforming reactor tube. Spanish Patent WO2015166129A1. 2014 Apr 30.

[5] Essoussi H, El Mouhri S, Ettaqi S, Essadiqi E. Heat treatment effect on mechanical properties of AISI 304 austenitic stainless steel. In: Moldovan L, Gligor A, editors. 12th International Conference Interdisciplinarity in Engineering-INTER-ENG; 2018 Oct 4-5; Tirgu Mures, Romania. Netherlands: Elsevier; 2019. p. 883-8.

[6] Xie L, Wang C, Wang Y, Wu G, Huang X. Grain size effect on the mechanical behavior of metastable Fe-23Cr-8.5Ni alloy. Metals. 2019;9(7):734.

[7] Ji HC, Li YM, Ma CJ, Long HY, Liu JP, Wang BY. Modeling of austenitic grain growth of 21-4N steel. Metalurgija. 2019;58(1-2):83-6.

[8] Krawczynska AT, Gierlotka S, Sucheck P, Setman D, Adamczyk-Cieslak B, Lewandowska M, et al. Recrystallization and grain growth of a nano/ultrafine structured austenitic stainless steel during annealing under high hydrostatic pressure. J Mater Sci. 2018;53:11823-36.

[9] Nasiri Z, Ghaemifar S, Naghizadeh M, Mirzadeh H. Thermal mechanisms of grain refinement in steels: a review. Met Mater Int. 2021;27(7):2078-94.

[10] Naghizadeh M, Mirzadeh H. Microstructural evolutions during annealing of plastically deformed AISI 304 austenitic stainless steel: martensite reversion, grain refinement, recrystallization, and grain growth. Metall Mater Trans A. 2016;47(8):4210-6.

[11] Sohrabi MJ, Naghizadeh M, Mirzadeh H. Deformation-induced martensite in austenitic stainless steels: a review. Archiv Civ Mech Eng. 2020;20(4):124.

[12] Järvenpää A, Jaskari M, Juuti T, Karjalainen P. Demonstrating the effect of precipitation on the mechanical stability of fine-grained austenite in reversion-treated 301LN stainless steel. Metals. 2017;7(9):344.

[13] Järvenpää A, Jaskari M, Kisko A, Karjalainen LP. Processing and properties of reversion-treated austenitic stainless steels. Metals. 2020;10(2):281.

[14] Tikhonova M, Belyakov A, Kaibyshev R. Static grain growth in an austenitic stainless steel subjected to intense plastic straining. In: Mishra B, Ionescu M, Chandra T, editors. The 8th International Conference on Processing and Manufacturing of Advanced Materials-THERMEC2013; 2013 Dec 2-6; Las Vegas, USA. Switzerland: Trans Tech Publications; 2014. p. 1021-6.

[15] Naghizadeh M, Mirzadeh H. Elucidating the effect of alloying elements on the behavior of austenitic stainless steels at elevated temperatures. Metall Mater Trans A. 2016;47(12):5698-703.

[16] Stanley JK, Perrotta AJ. Grain growth in austenitic stainless steels. Metallography. 1969;2(4):349-62.

[17] Dong D, Chen F, Cui Z. Modeling of austenite grain growth during austenitization in a low alloy steel. J Mater Eng Perform. 2016;25(1):152-64.

[18] Sellars CM, Whiteman JA. Recrystallization and grain growth in hot rolling. Metal Sci. 1979;13(3-4):187-94.

[19] Hall EO. The deformation and aging of mild steel: III discussion of results. Proc Phys Soc B. 1951;64(9):742.

[20] Huang YC, Su CH, Wu SK, Lin C. A study on the Hall-Petch relationship and grain growth kinetics in FCC-structured high/medium entropy alloys. Entropy. 2019;21(3):297.

[21] Gao Y, Ding Y, Chen J, Xu J, Ma Y, Wang X. Effect of twin boundaries on the microstructure and mechanical properties of Inconel 625 alloy. Mater Sci Eng A. 2019;767:138361.

[22] Li X, Wei Y, Wei Z, Zhou J. Effect of cold rolling on microstructure and mechanical properties of AISI 304N stainless steel. IOP Conf Ser Earth Environ Sci. 2019;252:022027.

[23] Poddar D, Chakraborty A, Kumar BR. Annealing twin evolution in the grain growth stagnant austenitic stainless steel microstructure. Mater Charact. 2019;155(11):109791.

[24] Naghizadeh M, Mirzadeh H. Effects of grain size on mechanical properties and work hardening behavior of AISI 304 austenitic stainless steel. Steel Res Int. 2019;90(10):1900153.

[25] Karmakar A, Kundu S, Roy S, Neogy S, Srivastava D, Chakrabarti D. Effect of microalloying elements on austenite grain growth in Nb-Ti and Nb-V steels. Mater Sci Technol. 2014;30(6):653-64.
[26] Ghosh D. Effects of grain size and nitrogen content on tensile flow properties of 316LN stainless steel at 300 K and 823 K [thesis]. Mumbai: Indian Institute of Technology Bombay; 2016.
[27] Nie Z, Wang G, Zhang Y, Rong Y. Experimental study and modelling on the grain growth of annealing process in Fe-50%Ni alloy. TMS 2015 144th Annual meeting & exhibition, annual meeting supplemental proceedings; 2015 Mar 15-19; Orlando, USA. Switzerland: Springer; 2016.
[28] Kim BN, Hiraga K, Morita K. Kinetics of normal grain growth depending on the size distribution of small grains. Mater Trans. 2003;14(11):2239-44.
[29] Chen S, Tseng KK, Tong Y, Li W, Tsai CW, Yeh JW, et al. Grain growth and Hall-Petch relationship in a refractory HfNbTaZrTi high-entropy alloy. J Alloys Compd. 2019;795(5):19-26.